Water Decomposition Occurring During Laser Breakdown of Aqueous Solutions Containing Individual Gold, Zirconium, Molybdenum, Iron or Nickel Nanoparticles

Ilya V. Baimler[1], Andrey B. Lisitsyn[2] and Sergey V. Gudkov[1]*

[1]Prokhorov General Physics Institute of the Russian Academy of Sciences, Moscow, Russia, [2]V. M. Gorbatov Federal Research Center for Food Systems of the Russian Academy of Sciences, Moscow, Russia

Generation rates of hydrogen peroxide (H_2O_2), hydroxyl radicals ($^{\bullet}OH$), molecular hydrogen (H_2), and molecular oxygen (O_2) forming during the optical breakdown of aqueous colloidal solutions containing Au, Mo, Zr, Fe, and Ni nanoparticles have been studied. It is shown that the processes occurring during the dissociation of water molecules under the influence of laser breakdown plasma and leading to the formation of various chemical products depend on the material of the nanoparticles present in the colloid. It was found that the highest rates of generation of water decomposition products are observed in aqueous colloidal solutions of Fe and Ni nanoparticles. The use of Au nanoparticles leads to the lowest generation rate. In general, the materials from which the nanoparticles are made, depending on the efficiency of the formation of water decomposition products, are arranged as follows: Ni> Fe> Mo> Zr> Au.

Keywords: laser radiation, nanoparticles, optical breakdown, hydrogen peroxide, hydroxyl radicals, molecular hydrogen, molecular oxygen

INTRODUCTION

The processes occurring under the action of high-power laser radiation on a matter has been actively studied since the creation of the first high-power lasers. Nowadays, the optical breakdown of liquids is intensively studied [1–3]. This topic is mainly associated with laser ablation technologies in liquids [4–6] and Laser-Induced Breakdown Spectroscopy (LIBS) technology [7–9].

It is known that the intensity of the processes occurring during the optical breakdown of liquids can increase significantly when nanoparticles are added to the liquid. For example, it has been shown that the rate of generation of H_2 and O_2 during optical breakdown of a liquid containing nanoparticles increases significantly [10, 11]. In the case of optical breakdown in the presence of gold nanoparticles in water, the rate of generation of hydroxyl radicals increases by almost two orders of magnitude [12]; similar results were obtained for hydrogen peroxide. It was found that the rate of generation of water decomposition products is significantly affected by the concentration of nanoparticles in an aqueous solution.

Usually, the dependence of the optical breakdown efficiency on the concentration of nanoparticles has one extremum, although there are also more complex dependencies [13]. Therefore, in this work, we used the same concentration of nanoparticles for all experimental groups. It is also known that the efficiency of optical breakdown is influenced by the size of nanoparticles present in a colloidal

FIGURE 1 | Scheme of the experimental setup. 1) Nd:YAG laser, λ = 1,064 nm, τ = 100 ns, ν = 10 kHz, 2) Laser radiation, 3) Motorized system of reflecting mirrors and lenses, 4) Cuvette with an aqueous solution of nanoparticles, 5) H_2 and O_2 analyzer.
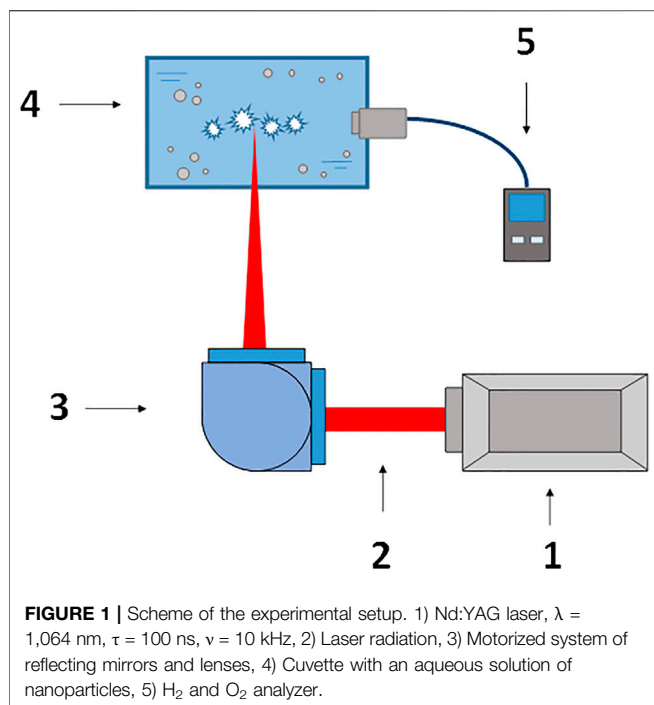
solution [14]. Thus, in this work, we used nanoparticles of close sizes for all experimental groups. It is known that the rate of formation of hydrogen peroxide, molecular hydrogen, or molecular oxygen during the ablation of massive targets from different metals differs significantly [15]. It is assumed that the rate of generation of water decomposition products is directly related to the redox potential of the target's material. It can be assumed that the effect of the nanoparticle material on the generation of water decomposition products can also be associated with the redox potential; however, unlike metals, nanoparticles often have an oxide layer on the surface [16]. Such a layer can even occur on gold [17] and other inert materials [18]. The surface oxide layer of a nanoparticle does not allow estimating its redox potential with the required accuracy, although researches in this area are being intensively conducted [19].

To date, there is insufficient information on the effect of the nanoparticle material on the processes accompanying laser breakdown in colloidal systems. In this regard, the aim of this work is to identify and characterize the effect of the nanoparticle material on the processes accompanying laser breakdown in colloidal systems. The study was carried out using the most similar transition metals of fourth periods (Fe, Ni) and fifth periods (Zr, Mo). Gold, The sixth period transition element, was used as a comparison. Gold is a good marker for comparison due to its relative inertness and widespread prevalence in studies.

METHODS

Nanoparticles of various metals were obtained by laser ablation in a liquid, details were published earlier [20, 21]. The size distribution and concentration of nanoparticles in the resulting colloids were determined using a CPS disc centrifuge. In the experiments, nanoparticles with the following average sizes were used: Au - 23 ± 3 nm, Zr - 20 ± 5 nm, Mo - 25 ± 3 nm, Fe - 29 ± 3 nm, Ni - 22 ± 2 nm. The nanoparticles had a metal core. An oxide layer with a thickness of no more than several nanometers was observed on the surface of nanoparticles.

The experimental setup is shown in **Figure 1**. A Nd: YAG laser with a wavelength λ = 1,064 nm, pulse duration τ = 10 ns, frequency ν = 10 kHz, average pulse energy ε = 1.25 mJ was used as a source of laser radiation. The laser beam was focused inside the cuvette using a motorized system of lenses and mirrors and moved along a fixed direction. Moving the laser beam is necessary for the following reason. Previously, we found that optical breakdown on individual nanoparticles occurs only in an undisturbed medium. After optical breakdown, the laser pulse cannot make a breakdown in the same place for several tens of microseconds; this is due to the emergence of air bubbles and thermal defocusing. Amperometric sensors of molecular oxygen and hydrogen connected to portable analyzers were mounted inside the cuvette. The experimental cuvette was filled with 20 ml deionized water. The cuvette was cooled externally, 20 ml is the optimal volume for temperature control and measurements. Then, nanoparticles of a certain metal were added to the cuvette to a final concentration of $n = 10^{10}$ pcs/ml. Earlier, we found that at a given concentration of nanoparticles in aqueous solutions, the highest rate of formation of water decomposition products is observed [22]. During irradiation of the colloidal solution of nanoparticles, the concentration of molecular hydrogen and molecular oxygen dissolved in the water was recorded.

Registration of hydrogen peroxide was carried out immediately after exposure to laser radiation. About 1 ml of colloidal solution was taken from the experimental cuvette. The hydrogen peroxide concentration was measured using the enhanced chemiluminescence method in the luminol-4-iodophenol-horseradish peroxidase system. We used a highly sensitive luminometer Biotoks 7A USE (ultra-sensitive edition). All experimental details were described earlier [23].

The concentration of short-lived hydroxyl radicals was measured using a coumarin-3-carboxylic acid (CCA) fluorescent probe. When molecules of hydroxyl radicals interact with molecules of coumarin-3-carboxylic acid, 7-OH-coumarin-3-carboxylic acid is formed with intense fluorescence (λ_{ex} = 410 nm, λ_{em} = 475 nm). The fluorescence response was measured using a high-sensitivity spectrofluorimeter. All experimental details were described earlier [22].

RESULTS AND DISCUSSION

Figure 2A shows the concentration dependence of molecular oxygen on the irradiation time of colloidal solutions of Au, Zr, Mo, Fe, and Ni nanoparticles. As can be seen from the figure, the concentration of molecular oxygen in the experimental cuvette does not undergo any changes during the first few minutes. After the onset of equilibrium between the mixture of atmospheric
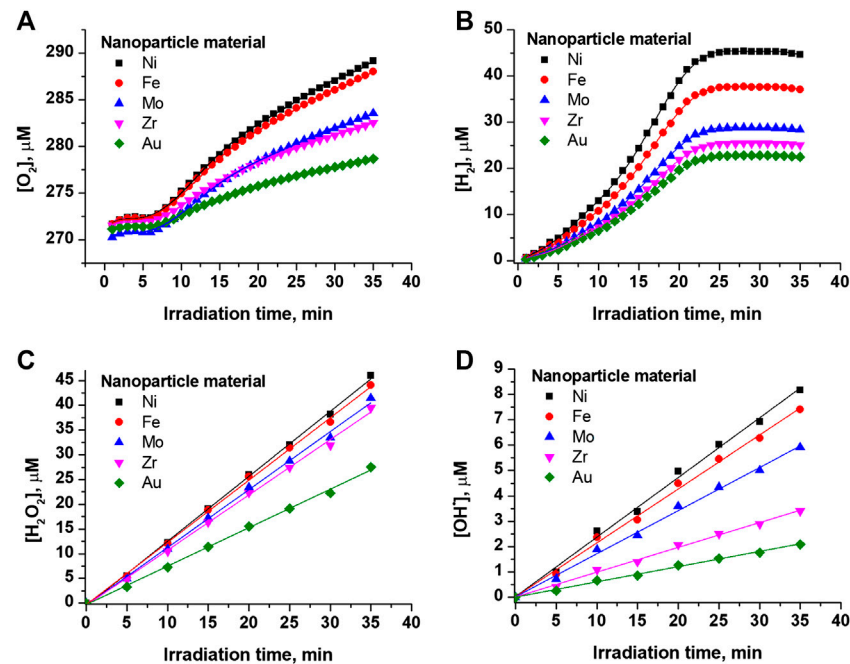
FIGURE 2 | Concentration change vs. irradiation time of the colloidal solution of nanoparticles **(A)** molecular oxygen **(B)** molecular hydrogen **(C)** hydrogen peroxide **(D)** hydroxyl radicals.

gases (N_2 + O_2) and newly formed gases (H_2 + O_2), the concentration of molecular oxygen in the colloid begins to monotonically increase with the time of irradiation. The slope of the straight line was used to calculate the rate of formation of molecular oxygen. Approximating the area in the interval from 10 to 15 min, which corresponds to the maximum slope i.e., the maximum rate of generation of molecular oxygen.

The concentration dependence of molecular hydrogen on the time of irradiation of colloidal solutions of Au, Zr, Mo, Fe, and Ni nanoparticles was studied, **Figure 2B**. The presented dependencies are characterized by nonlinear curves with a monotonic increase in concentration throughout the entire exposure time. The rate of generation of molecular hydrogen was determined from the slope of a straight line approximating a part of the experimental curve in the interval from 10 to 20 min. As can be seen from **Figure 2B**, the generation rate of molecular hydrogen is maximum when using nickel nanoparticles, and minimum when using gold nanoparticles.

Figure 2C shows the concentration dependence of hydrogen peroxide on the time of irradiation of the colloid. As can be seen from the figure, the dependence of the concentration of hydrogen peroxide on time has a linear form. The dependencies corresponding to different materials of nanoparticles are characterized by different rates of generation of hydrogen peroxide. It is shown that a high rate of hydrogen peroxide generation is observed upon irradiation of colloidal solutions of nickel nanoparticles. The lowest rate of hydrogen peroxide generation is observed upon irradiation of Au nanoparticles.

Figure 2D demonstrates the concentration dependence of hydroxyl radicals on the time of irradiation. The presented dependencies are approximated by straight lines with different slopes corresponding to a certain material of nanoparticles. Just as in the case of hydrogen peroxide, the highest rate of generation of hydroxyl radicals is observed upon irradiation of nickel nanoparticles, and the lowest—for gold nanoparticles.

It was found that the concentration of hydrogen peroxide and hydroxyl radicals increases linearly with the time of exposure to laser radiation. In contrast, the concentration of gases (molecular hydrogen and molecular oxygen) does not change linearly. At the initial stages, a lag phase is observed, with prolonged exposure, saturation is observed. It is obvious that the generation of gases during optical breakdown proceeds at the same rate; the change in the concentration of gases in a liquid is primarily associated with their solubility. At the initial stages, atmospheric gases (molecular nitrogen and molecular oxygen) are in the colloidal solution. Molecular oxygen and molecular hydrogen formed during optical breakdown begin to displace atmospheric gases from the system. In this case, molecular hydrogen displaces molecular oxygen and molecular nitrogen. In this regard, a quasi-equilibrium is formed in the system, which is shifted toward the accumulation of gases in the system when molecular nitrogen is displaced [10]. At later stages of laser exposure, the concentration of gases reaches the solubility limit and saturation occurs.

Figure 3 shows the values of the generation rates of various products of water decomposition depending on the used material of nanoparticles. As can be seen from **Figure 3**, the presence of

FIGURE 3 | Influence of nanoparticle material on generation processes. **(A)** generation rates of hydrogen peroxide **(B)** generation rates of hydroxyl radicals **(C)** generation rates of molecular hydrogen **(D)** generation rates of molecular oxygen.
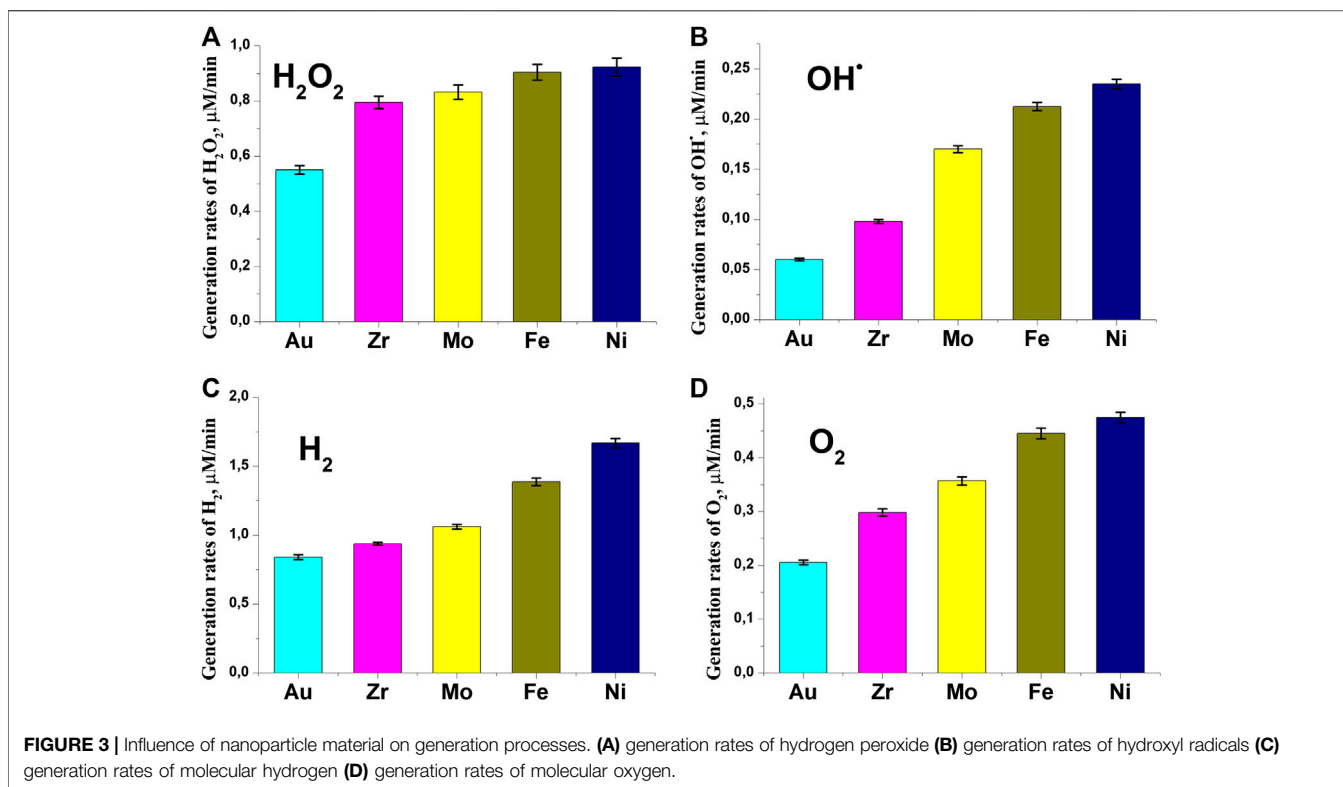
different nanoparticles in solution leads to different rates of generation of all products. Obviously, this is associated with an increase in the probability of a breakdown and, as a consequence, the number of breakdowns in the cell. The highest generation rates of all registered water decomposition products are observed when using colloidal solutions containing nickel nanoparticles, the lowest when using gold nanoparticles. The ratio of the rates of generation of $H_2/H_2O_2/O_2$ can, with some assumptions, be written as 4/2/1. From this it follows that for a certain number of water molecules, four hydrogen molecules, two hydrogen peroxide molecules and one oxygen molecule are formed.

It is interesting, that when all nanoparticles are used, the total equation of water decomposition has a form close to the following: $6H_2O \rightarrow 4H_2 + 2H_2O_2 + O_2$. This means that the nanoparticle material does not make a significant contribution to the overall balance of the equation. In other words, the material of nanoparticles does not substantially participate in the chemical transformations. Under the influence of various metals, the Fenton reaction (the reaction of decomposition of hydrogen peroxide) is most often observed: $H_2O_2 + Me \rightarrow$ $^-OH + {}^\bullet OH + Me^+$ [24].

In a separate series of experiments, the effect of the obtained nanoparticles was tested. Nanoparticles were added to a 100 μM hydrogen peroxide solution to a final concentration of 10^{10} pcs/ml and left for 30 min at 20°C. It was shown that all the nanoparticles used did not significantly affect the hydrogen peroxide concentration.

FIGURE 4 | Refractive index and absorption coefficient of metals at 1,064 nm wavelength. Data obtained from the database https://refractiveindex.info.
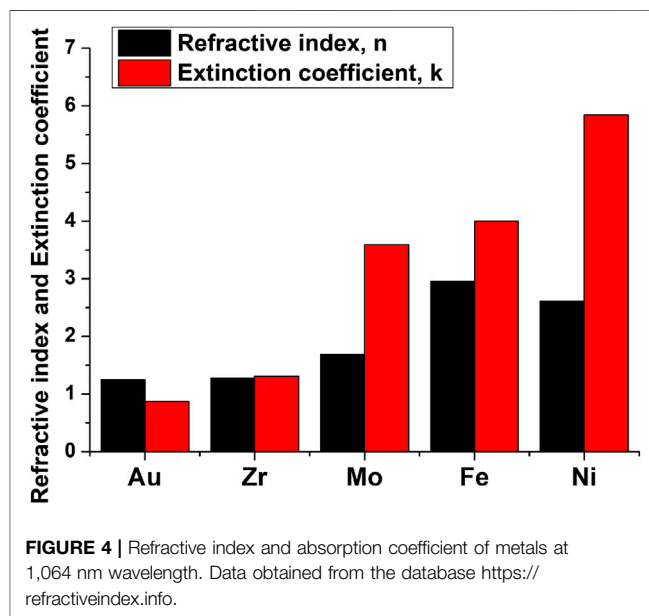
The greatest decomposition of hydrogen peroxide (about 10%) was recorded in colloidal solutions of iron and nickel nanoparticles. In principle, this result is predictable, since in the molar ratio in the colloid there were much fewer metal ions than hydrogen peroxide molecules.

The arrangement of the nanoparticle materials in the order presented can be explained by the difference in the absorption coefficient of the selected materials. Indeed, the fraction of radiation absorbed by a nanoparticle is determined by the absorption coefficient of the corresponding metal. With other parameters being equal, a larger amount of absorbed radiation leads to the formation of a breakdown plasma with a higher temperature and a larger localization region. As a result, the intensity of the decay of water molecules and the rate of formation of new chemical compounds are directly related to the fraction of the laser radiation energy absorbed by nanoparticles. The values for the absorption coefficient of each material at the radiation wavelengths of the laser used in the experiment (1,064 nm) are taken from ref. 25 and are shown in **Figure 4**. As one can see, the order in which the materials are arranged corresponds to that obtained in the experiment.

The discrepancies with the experimental data can be explained by the fact that the exact values of the absorption coefficients may differ for nanoparticles. It should also be taken into account that nanoparticle materials are mostly an oxide of a particular material, which also affects the value of the absorption coefficient.

CONCLUSION

The concentration dependencies of hydrogen peroxide, hydroxyl radicals, molecular hydrogen, and oxygen on the irradiation time of aqueous colloidal solutions of Au, Mo, Zr, Fe, and Ni nanoparticles have been investigated experimentally. It was found that when a fixed concentration of nanoparticles ($n = 10^{10}$ pcs/ml) is added to the solution and the resulting solution is irradiated, the rate of generation of

chemical products changes for various materials of nanoparticles. The observed changes in the generation rates, presumably, depend on the optical properties of a particular material and can change significantly during the oxidation of nanoparticles.

DATA AVAILABILITY STATEMENT

The raw data supporting the conclusions of this article will be made available by the authors, without undue reservation.

AUTHOR CONTRIBUTIONS

IB and SG conducted experiments. IB, AL, and SG participated in the processing of the results and their discussion. IB and SG participated in writing the text of the manuscript.

FUNDING

ACKNOWLEDGMENTS

REFERENCES

1. Kanitz A, Kalus M, Gurevich E, Ostendorf A, Barcikowski S, Amans D. Review on experimental and theoretical investigations of the early stage, femtoseconds to microseconds processes during laser ablation in liquid-phase for the synthesis of colloidal nanoparticles. *Plasma Sources Sci. Technol* (2019) 28:103001. doi:10.1088/1361-6595/ab3dbe

2. Vogel A, Linz N, Freidank S, Paltauf G. Femtosecond-laser-Induced nanocavitation in water: implications for optical breakdown threshold and cell surgery. *Phys. Rev. Lett* (2008) 100:038102. doi:10.1103/PHYSREVLETT.100.038102

3. Lama J, Lombard J, Dujardin C, Ledoux G, Merabia S, Amans D. Dynamical study of bubble expansion following laser ablation in liquids. *Appl. Phys. Lett* (2016) 108:074104. doi:10.1063/1.4942389

4. Zhang D, Ranjan B, Tanaka T, Sugioka K. Multiscale hierarchical micro/nanostructures created by femtosecond laser ablation in liquids for polarization-dependent broadband antireflection. *Nanomaterials* (2020) 10(8):1573. doi:10. 1573. 10.3390/nano10081573

5. Fernández Arias M, Boutinguiza M, Del Val J, Covarrubias C, Bastias F, Gómez L, et al. Copper nanoparticles obtained by laser ablation in liquids as bactericidal agent for dental applications. *Appl. Surf. Sci* (2019) 507:145032. doi:10.1016/j.apsusc.2019.145032

6. Shih CY, Shugaev M, Wu C, Zhigilei L. The effect of pulse duration on nanoparticle generation in pulsed laser ablation in liquids: insights from large-scale atomistic simulations. *Phys. Chem. Chem. Phys* (2020) 22:7077–99. doi:10.1039/D0CP00608D

7. Hahn D, Omenetto N. Laser-Induced breakdown spectroscopy (LIBS), Part II: review of instrumental and methodological approaches to material analysis and applications to different fields. *Appl. Spectrosc* (2012) 66:347–419. doi:10.1366/11-06574

8. Sdvizhenskii P, Lednev V, Asyutin R, Grishin M, Tretyakov R, Pershin S. Correction: online laser-induced breakdown spectroscopy for metal-particle powder flow analysis during additive manufacturing. *J. Anal. At. Spectrom* (2020) 35:632. doi:10.1039/D0JA90010A

9. Lednev V, Sdvizhenskii P, Asyutin R, Tretyakov R, Grishin M, Stavertiy A, et al. *In situ* elemental analysis and failures detection during additive manufacturing process utilizing laser induced breakdown spectroscopy. *Optic Express* (2019) 27:4612–28. doi:10.1364/OE.27.004612

10. Barmina E, Simakin A, Shafeev G. Hydrogen emission under laser exposure of colloidal solutions of nanoparticles. *Chem. Phys. Lett* (2016) 655-656:35–8. doi:10.1016/j.cplett.2016.05.020

11. Sukhov I, Shafeev G, Barmina E, Simakin A, Voronov V, Uvarov O. Generation of hydrogen by laser irradiation of colloids of iron and beryllium in water. *Quant. Electron* (2017) 47:533–8. doi:10.1070/QEL16325

12. Simakin A, Astashev M, Baimler I, Uvarov O, Voronov V, Vedunova M, et al. The effect of gold nanoparticle concentration and laser fluence on the laser-induced water decomposition. *J. Phys. Chem. B* (2019) 123(8):1869–80. doi:10.1021/acs.jpcb.8b11087

13. Barmina E, Gudkov S, Simakin A, Shafeev G. Stable products of laser-induced breakdown of aqueous colloidal solutions of nanoparticles. *J. Laser Micro Nanoeng* (2019) 12:254–7. doi:10.2961/jlmn.2017.03.0014

14. Baimler I, Simakin A, Uvarov O, Volkov M, Gudkov S. Generation of hydroxyl radicals during laser breakdown of aqueous solutions in the presence of Fe and Cu nanoparticles of different sizes. *Phys. Wave Phenom* (2020) 28:107–10. doi:10.3103/S1541308X20020028

15. Kalus M, Lanyumba R, Lorenzo-Parodi N, Jochmann M, Kerpen K, Hagemann U, et al. Determining the role of redox-active materials during laser-induced water decomposition. *Phys. Chem. Chem. Phys* (2019) 21:18636–51. doi:10.1039/C9CP02663K

16. Ziefuss AR, Haxhiaj I, Müller S, Gharib M, Gridina O, Rehbock C, et al. The origin of laser-induced colloidal gold surface oxidation and charge density, and its role in oxidation catalysis. *J. Phys. Chem. C* (2020) 124:20981–90. doi:10.1021/acs.jpcc.0c06257

17. Batista L, Meader V, Romero K, Kunzler K, Kabir F, Bullock A, et al. Kinetic control of [AuCl$_4$]- photochemical reduction and gold nanoparticle size with hydroxyl radical scavengers. *J. Phys. Chem. B* (2019) 123:7204–13. doi:10.1021/acs.jpcb.9b04643

18. Nichols W, Sasaki T, Koshizaki N. Laser ablation of a platinum target in water. III. Laser-induced reactions. *J. Appl. Phys* (2006) 100:114913. doi:10.1063/1.2390642

19. Markham J, Young N, Batchelor-McAuley C, Compton R. Bipolar nano impact transients: controlling the redox potential of nanoparticles in solution. *J. Phys. Chem. C* (2020) 124:14043–53. doi:10.1021/acs.jpcc.0c03316

20. Serkov A, Barmina E, Shafeev G, Voronov V. Laser ablation of titanium in liquid in external electric field. *Appl. Surf. Sci* (2015) 348:16–21. doi:10.1016/j.apsusc.2014.12.139

21. Shafeev G, Rakov I, Ayyyzhy K, Mikhailova G, Troitskii A, Uvarov O. Generation of Au nanorods by laser ablation in liquid and their further elongation in external magnetic field. *Appl. Surf. Sci* (2018) 466:477–82. doi:10.1016/j.apsusc.2018.10.062

22. Gudkov S, Guryev E, Gapeyev A, Sharapov M, Bunkin N, Shkirin A, et al. Unmodified hydrated C60 fullerene molecules exhibit antioxidant properties, prevent damage to DNA and proteins induced by reactive oxygen species and protect mice against injuries caused by radiation-induced oxidative stress. *Nanomedicine* (2019) 15:37–46. doi:10.1016/j.nano.2018.09.001

23. Shtarkman I, Gudkov S, Chernikov A, Bruskov V. Formation of hydrogen peroxide and hydroxyl radicals in aqueous solutions of L-amino acids by the action of X-rays and heat. *Biofizika* (2008) 53:5–13. doi:10.1134/S0006350908010016

24. Fenton HJH. Oxidation of tartaric acid in presence of iron. *J. Chem. Soc. Trans* (1894) 65:899–910. doi:10.1039/ct8946500899

25. Polyanskiy MN. Refractive index database. Available from: https://refractiveindex.info (Accessed 20 October, 2020).

Conflict of Interest: The authors declare that the research was conducted in the absence of any commercial or financial relationships that could be construed as a potential conflict of interest.